Wetting and Molecular Orientation of 8CB on Silicon Substrates

Lei Xu and Miquel Salmeron
Materials Sciences Division, Lawrence Berkeley National Laboratory, University of California, Berkeley, California 94720

Sebastien Bardon
Laboratoire de Physique de La Matière Condensée, Collège de France, 11 Place Marcelin Berthelot, 75231 Paris, France
(Received 25 October 1999)

The wetting properties of 8CB (4′-*n*-octyl-4-cyanobiphenyl) on silicon wafers have been studied with scanning polarization force microscopy (SPFM). Layer-by-layer spreading of 8CB droplets is observed. With the help of the surface potential mapping capability of SPFM, we found that the molecular dipole of the first monolayer of 8CB is parallel to the surface. A layer of nearly vertical molecular dimers on top of the monolayer has an associated surface potential of 40 mV, which is attributed to a distortion of the dimer. The dimer distortion propagates to the subsequent smectic bilayers, producing an additional 7 mV potential increase in the second layer, 2 mV on the third, and ~1 mV on the fourth.

PACS numbers: 68.10.Gw, 61.16.Ch, 61.30.Gd, 68.45.Gd

The wetting and spreading properties of liquid crystals (LC) on solid substrates are of interest due to their use in display devices. In addition these interesting liquids provide a good testing ground for fundamental theories of wetting. The LC in our studies is 4′-*n*-octyl-4-cyanobiphenyl (8CB). It has been studied by optical microscopy [1], x-ray reflectivity [2,3], ellipsometry [3,4], second-harmonic generation [5], scanning tunneling microscopy [6], atomic force microscopy (AFM) [7], and surface forces apparatus [8]. Here we present new results using a novel AFM technique that allows us to study for the first time properties of liquid films with nanometer scale resolution in the surface plane (x, y directions), and with angstrom resolution in the direction normal to the surface (z). We show that, while many of the wetting properties of 8CB that have been determined in the scale of tens of micrometers are still valid at the nanometer scale, new ones related to the small dimensions of the droplets are revealed. More importantly, we have obtained simultaneously with the topographic images information on the molecular orientations of 8CB in the various layers, based on the changes in surface potential that originate from the molecular dipole orientations. This is the first time that wetting properties and molecular scale properties could be directly connected through high resolution imaging and spectroscopy.

Bulk 8CB exists in three phases. With increasing temperature, there is a transition at 21.5 °C from a crystalline to a smectic-*A* phase; at 33.5 °C, there is a second-order transition to a nematic phase; and at 40.5 °C, there is a weak first-order transition to an isotropic liquid [9]. In bulk, the 8CB molecules are paired into dimers (1.4 times longer than a single molecule) with antiparallel dipole moments. In the smectic-*A* phase, the dimers form layers spaced by 31.7 Å, with the dimers aligned perpendicular to the layers [10]. Ellipsometry and x-ray reflectivity have been used to study the spreading and structure of macroscopic (in x, y) films of 8CB on silicon wafers [3,11]. It was found that a prewetting film is formed during spreading in the smectic and nematic phases. The prewetting film is composed of a monolayer of single 8CB molecules with a thickness of 8 Å, connected to a 41 Å thick film. This film consists of a ~33 Å thick bilayer on top of the 8 Å monolayer. Both monolayer and trilayer extend over millimeter distances. Because of the limited lateral resolution of the optical methods, details of the spreading and of the structure of these layers could not be studied.

High lateral resolution imaging in the nanometer range can be achieved using scanning probe microscopy methods, in particular, AFM. Contact and tapping AFM modes provide lateral resolution equal to the contact diameter, typically around 1 nm. Tapping mode AFM has indeed been used to image the prewetting layer [11]. However, the perturbation introduced by the contact severely limits the usefulness of the information obtained. Scanning polarization force microscopy (SPFM) is a noncontact AFM technique based on electrical forces. When imaging in this mode, the tip remains far above the surface (10–30 nm), so that perturbations can be minimized. This is done at the cost of lateral resolution, which is in the 10 nm range and still far better than achievable with optical methods. SPFM is performed with either dc or ac bias, which gives the technique spectroscopic capabilities [12]. By controlling the lever oscillation amplitude at the second harmonic of the driving frequency (2ω) and at the same time measuring the first harmonic (1ω) amplitude, simultaneous topographic and contact potential maps of the surface can be obtained. We use this method extensively in this study. SPFM has been successfully applied in studies of wetting [13,14], as shown in several examples. These include the wetting of aqueous solutions [15], the corrosion of aluminum by sulfuric acid [16], and the effects of disjoining pressure on the shape of submicrometer glycerol droplets [17].

The experiments were carried out in an AFM apparatus enclosed in a box, in which the relative humidity was

kept constant at the ambient value of ~35%. Although we did not study the effect of humidity on molecular orientation, they are known to be negligible in the case of silicon substrates [18]. Details of the setup have been described in previous papers [13,19]. A resistor connected to the sample holder is used to raise the temperature by passing current through it. The substrate is a silicon (111) sample covered by its native oxide. Prior to the experiments, the samples were cleaned with an ethanol solution. Contact AFM images revealed a very flat (~4 Å rms) surface over micrometer ranges.

To study the wetting properties of smectic-phase 8CB, a small amount of liquid was directly deposited on the substrate. For studies of the nematic and isotropic phases, 8CB was condensed from its vapor while keeping the Si substrate at the appropriate temperature (the vapor was produced by heating an 8CB reservoir to 80 °C in front of the substrate). When studying the spreading of submicrometer size deposits of 8CB, we observed a behavior similar to that found at macroscopic scales [3]: 8CB forms droplets and pancakes on the surface in the smectic phase, wets the surface in the nematic phase, and dewets it in the isotropic phase. However, we found that rapid cooling to room temperature, combined with the high viscosity of 8CB, freezes the liquid in the phase corresponding to the substrate temperature during deposition for days. For that reason, we concentrate on studies at room temperature. (Unless otherwise indicated, all SPFM images presented in this paper were obtained at room temperature.)

Molecular multilayer spreading could be observed with SPFM. This is shown in the top image in Fig. 1, which was obtained near the edge of a large spreading drop. It shows a layered structure with 32 Å steps (all z values have an associated error bar of ± 1 Å), the thickness of a smectic bilayer. The cross section in the middle of Fig. 1, taken in the direction of the arrow shown in the top image, shows the perfect layering of the smectic bilayers. Such layering near the edge of a spreading droplet has never been observed before. In a sequence of time-lapsed images, the layers can be seen advancing in the direction of the arrow at an average speed of 2–3 nm/s at room temperature. The layers advance on top of the prewetting trilayer, which extends over very large distances (mm) in front of the droplet. Although the stable state of 8CB on silicon is in the form of a pancake, we observed metastable nanometer-scale droplets surrounded by layered structures. The bottom image in Fig. 1 shows an example of this. The shape of the droplet is not spherical. A higher resolution image shows that the lower part of the droplet is also layered with steps 32 Å high.

The vapor deposition method at variable substrate temperature provides additional insight into the structure and wetting properties of 8CB in its various phases. If the substrate temperature is between 41 and 33 °C, flat islands of 32 Å thickness are formed if only a small amount of 8CB is condensed on the surface. The size of these flat islands

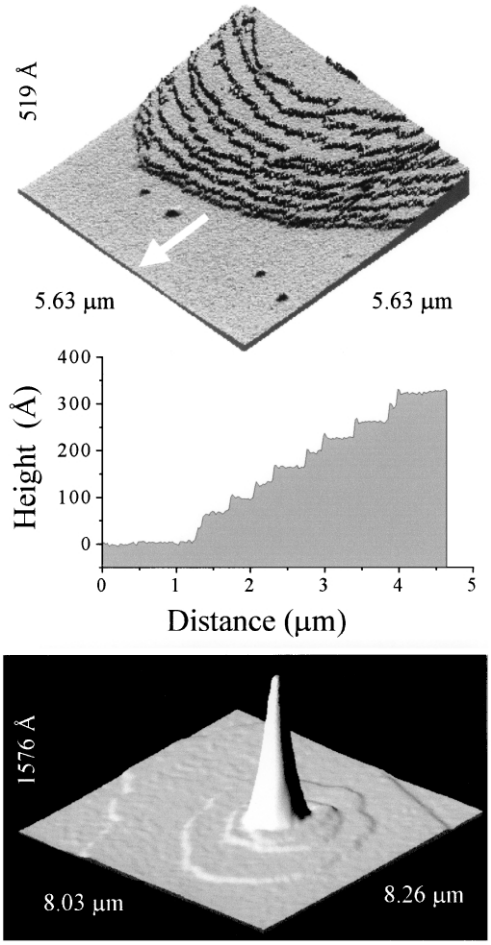

FIG. 1. Top: SPFM image of the spreading front of a large smectic drop of 8CB liquid crystal on a Si wafer, showing a layered structure. Each layer is 32 Å thick, as shown in the cross section in the middle. The layers advance in the direction of the arrow at the rate of 2–3 nm/s at room temperature. Bottom: Drop and surrounding smectic layers.

increases with deposition time while their height remains constant until a uniform layer is formed. If more 8CB is deposited, droplets form on top of the film. This is shown in the right image in Fig. 2.

On samples prepared with a substrate temperature above 41 °C, only spherical droplets were observed. Although no change could be observed in the droplets for several days, we noticed that, by applying a strong attractive electrostatic force (produced by a high bias or a small tip-surface distance), the tip could induce the droplets to spread and form pancakes. This indicates that the droplets are indeed in a metastable state.

To determine whether the 8CB droplets condensed above 41 °C (trapped in the isotropic phase) sit on a trilayer or on bare silicon, we used the AFM tip to mechanically spread the droplets and thus accelerate their conversion to a stable configuration. The SPFM images shown in Fig. 3 were obtained after such tip-induced spreading. After spreading, a layered structure with

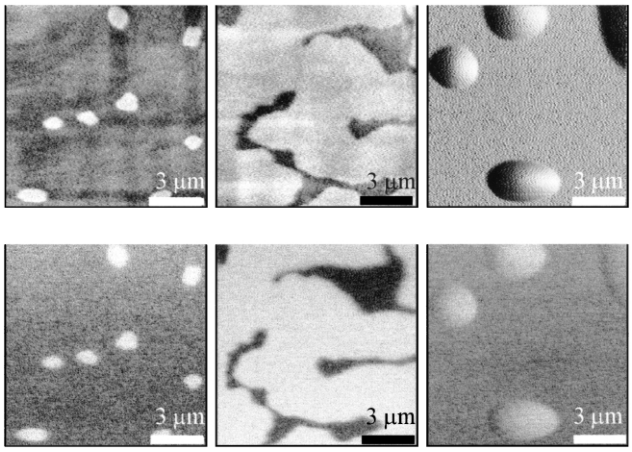

FIG. 2. Top: SPFM topographic images showing various stages of the vapor deposited 8CB film on a Si substrate at a temperature between 33 and 41 °C. The evaporation time increases from seconds to minutes from the left to the right images. Flat 32 Å thick islands grow until they cover the substrate completely. Further deposition produces droplets on top of the flat film. Bottom: Simultaneously acquired contact potential images. They gray scale is proportional to the local surface potential. On the islands, the potential is 40 mV higher than that of the outside. On the drops, the potential is 10 mV higher than that of the surrounding area.

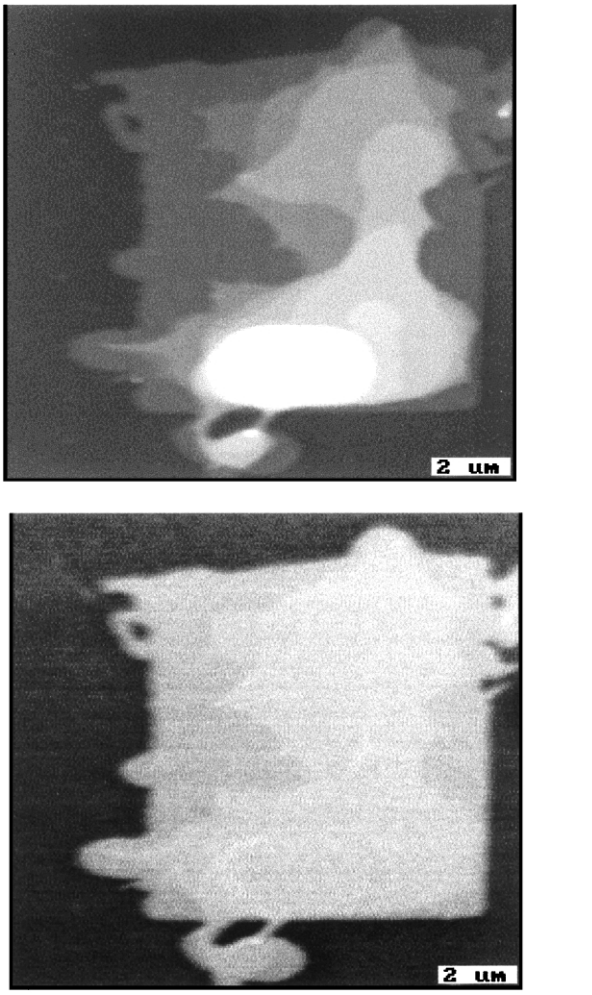

FIG. 3. Top: SPFM image obtained after spreading an 8CB droplet on silicon by contact with the AFM tip scanning over a square area. Several layers can be observed. The first one is 41 Å high and the following ones are 32 Å thick. The bright spot near the bottom is the remaining unspread droplet. Bottom: Simultaneously acquired contact potential image. The potential in the first layer is 40 mV higher than that of the substrate and the potential of the second layer is 7 mV higher than that of the first. The third and fourth layer potentials are 2 and 1 mV higher, respectively. Above that, the increase is negligible.

$\sim$32 Å high steps typical of the smectic phase is obtained. The first or bottom layer is 41 Å thick, while the layers above it are all 32 Å thick. This indicates that the bottom layer of the film is a trilayer and that the remaining substrate is dry silicon, i.e., not covered with either a monolayer or a trilayer of 8CB. We can thus conclude that the frozen isotropic droplets sit on the bare silicon surface. By contrast, the flat layer of Fig. 2, formed by evaporation between 33 and 41 °C, is 32 Å high, indicating that it consists of a bilayer on top of the monolayer. The monolayer must have formed very rapidly during the first stages of exposure to the vapor.

The simultaneously acquired contact potential images provide important structural information on the liquid film. The droplets formed at temperatures $>$41 °C have a surface potential 50 mV ($\pm$3) higher than the surrounding background (not shown). The 32 Å film formed between 41 and 33 °C has a potential about 40 mV higher than the surrounding monolayer and the droplets formed above that film have a potential 10 mV higher than the bilayer film (Fig. 2). In the structure formed after tip spreading, the bottom trilayer has a surface potential 40 mV higher than the surrounding substrate while the bilayer above it is 7 mV more positive. The third bilayer adds 2 mV and the fourth adds $\sim$1 mV. Layers above the fourth make negligible contributions. The total potential increase, at the top of pancakes or multilayers, is $\sim$50 mV higher than that of the bare silicon substrate, which is similar to that of the frozen isotropic droplets. This indicates that the isotropic droplets have similarly oriented bottom layers, with the remaining 8CB molecules above them not contributing to the droplet potential.

The information obtained from the simultaneously acquired topographic and surface potential images allows us to propose a model for the structure of 8CB in various wetting situations. We have seen in Fig. 2 that the potential of the first bilayer (32 Å thick) is 40 mV higher than the monolayer it sits on. The same contact potential difference is measured between the trilayer (41 Å) and the bare silicon (Fig. 3). These two observations indicate that the monolayer bound to silicon does not contribute appreciably to the surface potential. This in turn indicates that the molecular dipole moment is parallel to the surface. Since

the dipole originates in the charge distribution between the nitrogen and benzene rings, only this part needs to be parallel to the surface. This is consistent with the 8 Å thickness of the monolayer observed by ellipsometry. The 8 Å is contributed by the alkane group at a $\sim 30^\circ$ with the surface, giving a height of 4 Å, plus the 4–5 Å of the flat-lying biphenyl group.

Since the 8CB dimers in the bulk have no net dipole moment, we conclude that the 40 mV of the first bilayer on top of the monolayer originates from a distortion of the 8CB pair that misaligns their dipoles so as to give a net value. One possible mechanism for that distortion is the van der Waals interaction between the alkane tail chains. This tends to make the chains in the monolayer (partially sticking up) parallel with the alkane chains of the next bilayer. This would affect one of the 8CB monomers in the dimer. To create a 40 mV potential change, the dipoles in the dimer must misalign on the order of $\sim 3^\circ$, if we use the known dipole moment of 8CB and the surface density given by the molecular dimensions. In subsequent bilayers, the distortion decays rapidly, as manifested by their decreasing contribution to the surface potential.

The 40 mV surface potential of the first bilayer is small when compared with the surface potential of an 8CB Langmuir-Blodgett (LB) monolayer film [7], where a value of 610 mV has been measured. The difference is explained by the fact that the molecules in the LB film are unpaired and almost perpendicular to the substrate, while in our case the monolayer has a negligible contribution and the surface potential is due to a small distortion of the dimer.

In conclusion, the application of novel high resolution imaging and spectroscopic techniques has provided new insight into the molecular structure and wetting of 8CB on silicon substrates. For the first time, the layer-by-layer spreading is observed. Surface potential mapping enabled us to determine the orientation of the molecular dipole moments. We found that the first monolayer of 8CB does not contribute to the surface potential, thereby indicating that it is bound with the molecular dipole parallel to the surface. The layer of molecular dimers on top of the monolayer has an associated surface potential of 40 mV, which we attribute to a distortion of the dimer. The dimer distortion propagates to subsequent smectic bilayers for an additional 10 mV potential increase after four layers. Finally, we found that small droplets of 8CB can be trapped into nematic or isotropic phases due to strong substrate interaction and slow kinetics.

We thank A.-M. Cazabat and M.-P. Valignat for helpful discussions. This work was supported by a Cooperative Research and Development Agreement (CRADA) with Seagate Technology through the Director, Office of Science, Office of Basic Energy Sciences, Materials Sciences Division of the U.S. Department of Energy under Contract No. DE-AC03-76SF00098.

[1] M. F. Grandjean, C.R. Acad. Sci. **166**, 165 (1917).
[2] P. S. Pershan, J. Phys. (Paris), Colloq. **50**, C7–1 (1989).
[3] S. Bardon, R. Ober, M. P. Valignat, F. Vandenbrouck, A. M. Cazabat, and J. Daillant, Phys. Rev. E **59**, 6808 (1999).
[4] M. P. Valignat, S. Villette, J. Li, R. Barberi, R. Bartolino, E. Dubois-Violette, and A. M. Cazabat, Phys. Rev. Lett. **77**, 1994 (1996).
[5] M. B. Feller, W. Chen, and Y. R. Shen, Phys. Rev. A **43**, 6778 (1991).
[6] F. Stevens, D. L. Patrick, V. J. Cee, T. J. Purcell, and T. P. Beebe, Jr., Langmuir **14**, 2396 (1998).
[7] J. Fang, C. M. Knobler, and H. Yokoyama, Physica (Amsterdam) **244A**, 91 (1997).
[8] A. Artsyukhovich, L. D. Broekman, and M. Salmeron, Langmuir **15**, 2217 (1999).
[9] O. Mondain-Monval, H. J. Coles, T. Claverie, J. R. Lalanne, J. P. Marcerou, and J. Philip, J. Chem. Phys. **101**, 6301 (1994).
[10] S. H. J. Idziak, C. R. Safinya, R. S. Hill, K. E. Kraiser, M. Ruths, H. E. Warriner, S. Steinberg, K. S. Liang, and J. N. Israelachvili, Science **264**, 1915 (1994).
[11] S. Bardon, M. P. Valignat, A. M. Cazabat, W. Stocker, and J. P. Rabe, Langmuir **14**, 2916 (1998).
[12] C. Schonenbergher and S. F. Alvarado, Phys. Rev. Lett. **65**, 3162 (1990).
[13] J. Hu, X.-D. Xiao, and M. Salmeron, Appl. Phys. Lett. **67**, 476 (1995).
[14] L. Xu, A. Lio, J. Hu, D. F. Ogletree, and M. Salmeron, J. Phys. Chem. B **102**, 540 (1998).
[15] M. Salmeron, L. Xu, J. Hu, and Q. Dai, MRS Bull. **22**, 36 (1997).
[16] Q. Dai, J. Hu, A. Freedman, G. N. Robinson, and M. Salmeron, in *Diagnostic Techniques for Semiconductor Materials Processing II*, edited by S. W. Pang, O. J. Glembocki, F. H. Pollak, F. G. Celii, and C. M. Sotomayor Torres (Materials Research Society, Pittsburgh, 1996), p. 215.
[17] L. Xu and M. Salmeron, J. Phys. Chem. B **102**, 7210 (1998).
[18] J. Bechhoefer, B. Jérôme, and P. Pieranski, Phys. Rev. A **41**, 3187 (1990).
[19] J. Hu, X.-D. Xiao, D. F. Ogletree, and M. Salmeron, Science **268**, 267 (1995).